Polarized Ultrashort Brilliant Multi-GeV γ Rays via Single-Shot Laser-Electron Interaction

Yan-Fei Li,[1,2] Rashid Shaisultanov,[2] Yue-Yue Chen,[2] Feng Wan,[1,2] Karen Z. Hatsagortsyan,[2,*] Christoph H. Keitel,[2] and Jian-Xing Li[1,2,†]

[1]*MOE Key Laboratory for Nonequilibrium Synthesis and Modulation of Condensed Matter, School of Science, Xi'an Jiaotong University, Xi'an 710049, China*

[2]*Max-Planck-Institut für Kernphysik, Saupfercheckweg 1, 69117 Heidelberg, Germany*

(Received 20 July 2019; revised manuscript received 28 September 2019; published 9 January 2020)

Generation of circularly polarized (CP) and linearly polarized (LP) γ rays via the single-shot interaction of an ultraintense laser pulse with a spin-polarized counterpropagating ultrarelativistic electron beam has been investigated in nonlinear Compton scattering in the quantum radiation-dominated regime. For the process simulation, a Monte Carlo method is developed which employs the electron-spin-resolved probabilities for polarized photon emissions. We show efficient ways for the transfer of the electron polarization to the high-energy photon polarization. In particular, multi-GeV CP (LP) γ rays with polarization of up to about 95% can be generated by a longitudinally (transversely) spin-polarized electron beam, with a photon flux meeting the requirements of recent proposals for the vacuum birefringence measurement in ultrastrong laser fields. Such high-energy, high-brilliance, high-polarization γ rays are also beneficial for other applications in high-energy physics, and laboratory astrophysics.

DOI: 10.1103/PhysRevLett.124.014801

Polarization is a crucial intrinsic property of a γ photon. In astrophysics the γ-photon polarization provides detailed insight into the γ-ray emission mechanism and on properties of dark matter [1,2]. Highly polarized high-energy γ rays are a versatile tool in high-energy [3] and nuclear physics [4]. For instance, polarized γ rays of tens of MeV can be used to excite polarization-dependent photofission of the nucleus in the giant dipole resonance [5], while polarized γ rays of up to GeV play crucial roles for the meson photoproduction [6].

Recently, several proposals have been put forward to detect vacuum birefringence in ultrastrong laser fields, probing it with circularly polarized (CP) or linearly polarized (LP) γ photons of high-energies (larger than MeV and up to several GeV), see [7–11], taking advantage of the fact that the QED vacuum nonlinearity is significantly enhanced for high-energy photons. As proved in [11], the use of CP rather than LP probe photons reduces the measurement time of vacuum birefringence and vacuum dichroism by two orders of magnitude.

The common ways of producing high-energy polarized γ rays are linear Compton scattering [12–16] and bremsstrahlung [17–20]. The advantage of the former is that it employs unpolarized electron beams, and the emitted γ-photon polarization is determined by the driving laser polarization, while in the latter the spin of the scattering electron determines the γ-photon polarization [21]. However, in linear Compton scattering the electron-photon collision luminosity is rather low. The collision luminosity can be increased by using high-intensity lasers, but in this case the interaction regime moves into the nonlinear regime, when the radiation formation length is much smaller than the laser wavelength. Then during the photon formation the laser field does not vary much and the emission process acquires similarity to bremsstrahlung. Namely, in the nonlinear regime the circular polarization of the emitted γ photon requires longitudinally spin-polarized (LSP) electrons. Nevertheless, the nonlinear regime of Compton scattering is beneficial for the generation of polarized γ photons, because the polarization is enhanced at high γ-photon energies [12], and the typical emitted photon energy is increased in the quantum nonlinear regime, becoming comparable with the electron energy [22,23]. In the nonlinear regime the relative bandwidth of emission is increased [24], which is not suitable for photonic applications involving narrow resonances, and stimulated investigations for the bandwidth reduction, see, e.g., [25,26]. However, vacuum birefringence is not a resonant effect and its measurement does not require a small γ-photon bandwidth, but mostly high flux of highly polarized high-energy photons.

Regarding deficiencies connected with the bremsstrahlung mechanism, the incoherent bremsstrahlung cannot generate LP γ photons, and the scattering angle and emission divergence are both relatively large [27]. Furthermore, for coherent bremsstrahlung [4,28], the current density of the impinging electrons and the radiation flux is limited by the damage threshold of the crystal material [20,29,30].

With rapid developments of strong laser techniques, stable (energy fluctuation ~1%) ultrashort, ultraintense laser pulses can reach peak intensities of the scale of 10^{22} W/cm^2 with a duration of about tens of femtoseconds [31–36], opening new ways to generate high-energy, high-flux γ rays [37–42] in the nonlinear regime of Compton scattering [22,43–45]. Moderately polarized γ photons have been predicted in strong fields in electron-spin-averaged treatment [7,46,47]. However, the polarization properties of radiation are essentially spin dependent in the nonlinear regime [27,48], differing from those in the linear regime [49–52]), which calls for comprehensive spin-resolved studies, especially in the most attractive high-energy regime.

In this Letter, the feasibility of generation of polarized ultrashort multi-GeV brilliant γ rays via nonlinear Compton scattering with spin-polarized electrons is investigated theoretically (see Fig. 1). High-flux γ photons with polarization beyond 95% are shown to be feasible in a single-shot interaction, along with new applications in high-energy, astro-, and strong-laser physics. The investigation is based on the developed Monte Carlo method for simulation of polarization-resolved radiative processes in the interaction of an ultrastrong laser beam with a relativistic spin-polarized electron beam. While the scheme for CP γ photons includes an arbitrarily polarized (AP) laser pulse colliding with a LSP electron bunch [see Fig. 1(a)], the scheme for LP γ photons employs an elliptically polarized (EP) laser pulse with a small ellipticity colliding with a transversely spin-polarized (TSP) electron bunch [see Fig. 1(b)]. The spin-dependent radiation reaction in a laser field with a small ellipticity yields the separation of γ photons with respect to the polarization and the enhancement of the polarization rate.

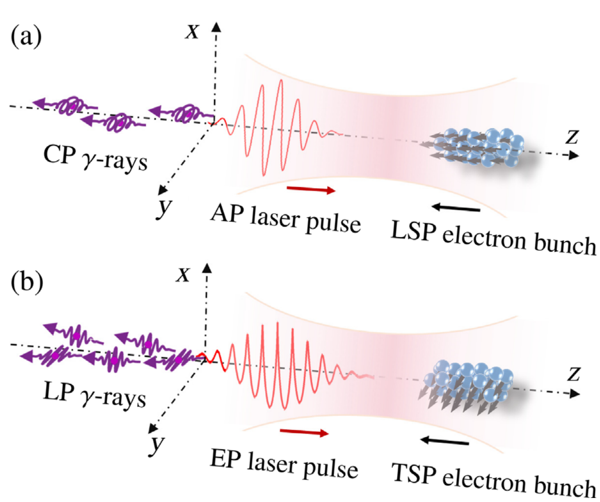

FIG. 1. Scenarios of generating CP and LP γ rays via nonlinear Compton scattering. (a) An arbitrarily polarized (AP) laser pulse propagating along $+z$ direction and head-on colliding with a longitudinally spin-polarized (LSP) electron bunch produces CP γ rays. (b) An elliptically polarized (EP) laser pulse propagating along $+z$ direction and colliding with a transversely spin-polarized (TSP) electron bunch produces LP γ rays. The major axis of the polarization ellipse is along the x axis.

Let us first introduce our new Monte Carlo method for simulation of polarized γ-photon emissions during the interaction of polarized relativistic electrons with ultrastrong laser fields. Photon emissions are treated quantum mechanically, while the electron dynamics semiclassically. At each simulation step the photon emission is determined by the total emission probability, and the photon energy by the spectral probability, using the common algorithms [53–55]. The spin of the electron after the emission is determined by the spin-resolved emission probabilities according to the algorithm of Ref. [56] and instantaneously collapsed into one of its basis states defined with respect to the instantaneous spin quantization axis (SQA), which is chosen according to the particular observable of interest; for more details, see the Supplemental Material [57]. For determination of the photon polarization, we employ the polarized photon emission probabilities by polarized electrons in the local constant field approximation [22,27,58–62], which are derived in the Baier-Katkov QED operator method [63]. This approximation is valid in ultrastrong laser field, when the invariant field parameter is large $a_0 \equiv |e|E_0/(m\omega_0) \gg 1$ [22,27], with laser field amplitude E_0, frequency ω_0, and the electron charge e and mass m. Relativistic units with $c = \hbar = 1$ are used throughout. The radiation probabilities are characterized by the quantum strong field parameter $\chi \equiv |e|\sqrt{-(F_{\mu\nu}p^\nu)^2}/m^3$ [22], where $F_{\mu\nu}$ is the field tensor, and p^ν the four-vector of the electron momentum. The angle-integrated radiation probability of a polarized photon with a polarized electron reads:

$$\frac{d^2W_{fi}}{dud\eta} = \frac{W_R}{2}(F_0 + \xi_1 F_1 + \xi_2 F_2 + \xi_3 F_3), \qquad (1)$$

where $W_R = \alpha m/[8\sqrt{3}\pi \lambdabar_c (k \cdot p_i)(1+u)^3]$, α is the fine structure constant, $u = \varepsilon_\gamma/(\varepsilon_i - \varepsilon_\gamma)$, $\lambdabar_c$ the Compton wavelength, ε_γ the emitted photon energy, ε_i the electron energy before radiation, $\eta = k \cdot r$ the laser phase, while p_i, k, and r are four-vectors of the electron momentum before radiation, laser wave vector, and coordinate, respectively. The photon polarization is represented by the Stokes parameters (ξ_1, ξ_2, ξ_3), defined with respect to the axes $\hat{\mathbf{e}}_1 = \hat{\mathbf{a}} - \hat{\mathbf{v}}(\hat{\mathbf{v}}\hat{\mathbf{a}})$ and $\hat{\mathbf{e}}_2 = \hat{\mathbf{v}} \times \hat{\mathbf{a}}$ [64], with the photon emission direction $\hat{\mathbf{n}}$ along the electron velocity $\mathbf{v}$ for the ultrarelativistic electron, $\hat{\mathbf{v}} = \mathbf{v}/|\mathbf{v}|$, and the unit vector $\hat{\mathbf{a}} = \mathbf{a}/|\mathbf{a}|$ along the electron acceleration $\mathbf{a}$. The variables introduced in Eq. (1) read:

$$\begin{aligned} F_0 = &-(2+u)^2[\mathrm{Int}K_{\frac{1}{3}}(u') - 2K_{\frac{2}{3}}(u')](1+\mathbf{S}_{if}) \\ &+ u^2(1-\mathbf{S}_{if})[\mathrm{Int}K_{\frac{1}{3}}(u') + 2K_{\frac{2}{3}}(u')] + 2u^2\mathbf{S}_{if}\mathrm{Int}K_{\frac{1}{3}}(u') \\ &-(4u+2u^2)(\mathbf{S}_f + \mathbf{S}_i)\cdot[\hat{\mathbf{v}} \times \hat{\mathbf{a}}]K_{\frac{1}{3}}(u') \\ &-2u^2(\mathbf{S}_f - \mathbf{S}_i)\cdot[\hat{\mathbf{v}} \times \hat{\mathbf{a}}]K_{\frac{1}{3}}(u') \\ &-4u^2[\mathrm{Int}K_{\frac{1}{3}}(u') - K_{\frac{2}{3}}(u')](\mathbf{S}_i \cdot \hat{\mathbf{v}})(\mathbf{S}_f \cdot \hat{\mathbf{v}}), \end{aligned} \qquad (2)$$

$$F_1 = -2u^2 \mathrm{Int}K_{\frac{1}{3}}(u')\{(\mathbf{S}_i\cdot\hat{\mathbf{a}})\mathbf{S}_f\cdot[\hat{\mathbf{v}}\times\hat{\mathbf{a}}] + (\mathbf{S}_f\cdot\hat{\mathbf{a}})\mathbf{S}_i\cdot[\hat{\mathbf{v}}\times\hat{\mathbf{a}}]\} + 4u[(\mathbf{S}_i\cdot\hat{\mathbf{a}})(1+u) + (\mathbf{S}_f\cdot\hat{\mathbf{a}})]K_{\frac{1}{3}}(u') + 2u(2+u)\hat{\mathbf{v}}\cdot[\mathbf{S}_f\times\mathbf{S}_i]K_{\frac{2}{3}}(u'), \quad (3)$$

$$F_2 = -(2u^2\{(\mathbf{S}_i\cdot\hat{\mathbf{v}})\mathbf{S}_f\cdot[\hat{\mathbf{v}}\times\hat{\mathbf{a}}] + (\mathbf{S}_f\cdot\hat{\mathbf{v}})\mathbf{S}_i\cdot[\hat{\mathbf{v}}\times\hat{\mathbf{a}}]\} + 2u(2+u)\hat{\mathbf{a}}\cdot[\mathbf{S}_f\times\mathbf{S}_i])K_{\frac{1}{3}}(u') - 4u[(\mathbf{S}_i\cdot\hat{\mathbf{v}}) + (\mathbf{S}_f\cdot\hat{\mathbf{v}})(1+u)] \times \mathrm{Int}K_{\frac{1}{3}}(u') + 4u(2+u)[(\mathbf{S}_i\cdot\hat{\mathbf{v}}) + (\mathbf{S}_f\cdot\hat{\mathbf{v}})]K_{\frac{2}{3}}(u'), \quad (4)$$

$$F_3 = 4\left[1+u+\left(1+u+\frac{u^2}{2}\right)\mathbf{S}_{if} - \frac{u^2}{2}(\mathbf{S}_i\cdot\hat{\mathbf{v}})(\mathbf{S}_f\cdot\hat{\mathbf{v}})\right]K_{\frac{2}{3}}(u') + 2u^2\{\mathbf{S}_i\cdot[\hat{\mathbf{v}}\times\hat{\mathbf{a}}]\mathbf{S}_f\cdot[\hat{\mathbf{v}}\times\hat{\mathbf{a}}] - (\mathbf{S}_i\cdot\hat{\mathbf{a}})(\mathbf{S}_f\cdot\hat{\mathbf{a}})\}\mathrm{Int}K_{\frac{1}{3}}(u') - 4u[(1+u)\mathbf{S}_i\cdot[\hat{\mathbf{v}}\times\hat{\mathbf{a}}] + \mathbf{S}_f\cdot[\hat{\mathbf{v}}\times\hat{\mathbf{a}}]]K_{\frac{1}{3}}(u'), \quad (5)$$

where $u' = 2u/3\chi$, $\mathrm{Int}K_{\frac{1}{3}}(u') \equiv \int_{u'}^{\infty} dz K_{\frac{1}{3}}(z)$, K_n is the n-order modified Bessel function of the second kind, $\mathbf{S}_i$ and $\mathbf{S}_f$ are the electron spin-polarization vector before and after radiation, respectively, $|\mathbf{S}_{i,f}| = 1$, and $\mathbf{S}_{if} \equiv \mathbf{S}_i \cdot \mathbf{S}_f$. Our Monte Carlo algorithm to determine the photon polarization yields the following, taking into account that the averaged polarization of the emitted photon is in a mixed state:

$$\xi_1^{\mathrm{mix}} = F_1/F_0, \quad \xi_2^{\mathrm{mix}} = F_2/F_0, \quad \xi_3^{\mathrm{mix}} = F_3/F_0. \quad (6)$$

Here we choose as the basis for the emitted photon [64,65] the two orthogonal pure states with the Stokes parameters $\hat{\boldsymbol{\xi}}^{\pm} \equiv \pm(\xi_1^{\mathrm{mix}}, \xi_2^{\mathrm{mix}}, \xi_3^{\mathrm{mix}})/\xi_0^{\mathrm{mix}}$ with $\xi_0^{\mathrm{mix}} \equiv \sqrt{(\xi_1^{\mathrm{mix}})^2 + (\xi_2^{\mathrm{mix}})^2 + (\xi_3^{\mathrm{mix}})^2}$.

Using the probabilities for the photon emission in these states $W_{fi}^{\pm}$ given by Eq. (1), we define the stochastic procedure with a random number $N_r \in [0, 1]$: if $W_{fi}^{+}/\bar{W}_{fi} \geq N_r$, the $\hat{\boldsymbol{\xi}}^{+}$ photon state is chosen, otherwise the photon state is set to $\hat{\boldsymbol{\xi}}^{-}$, see [57]. The Stokes parameters of each emitted photon are rotated from the instantaneous frame (ξ_1, ξ_2, ξ_3) defined with respect to the basis vectors $\hat{\mathbf{e}}_1$, $\hat{\mathbf{e}}_2$, and $\hat{\mathbf{n}}$ to the observation frame $(\xi_1^{(o)}, \xi_2^{(o)}, \xi_3^{(o)})$ defined with respect to the basis vectors $\hat{\mathbf{o}}_1$, $\hat{\mathbf{o}}_2$, and $\hat{\mathbf{o}}_3$, see [57,64]. Here, $\bar{W}_{fi} \equiv W_R F_0$ is the electron-spin-resolved radiation probability averaged by the photon polarization, cf. [56]. Averaging over the electron spin in Eq. (1) yields $\xi_2 = 0$, indicating that only LP γ-photons can be generated with unpolarized electrons, in accordance with [46].

The simulation results for the generation of CP γ rays are shown in Fig. 2. A realistic, tightly focused Gaussian LP laser pulse is used [57,66,67], with peak intensity $I_0 \approx 3.45 \times 10^{21}$ W/cm^2 ($a_0 = 50$), wavelength $\lambda_0 = 1$ μm, pulse duration $\tau = 10T_0$ with period T_0, and focal radius $w_0 = 5$ μm. The electron beam counterpropagating with the laser pulse (polar angle $\theta_e = 180°$ and azimuthal angle $\phi_e = 0°$) is fully LSP with $(\bar{S}_x, \bar{S}_y, \bar{S}_z) = (0, 0, -1)$. It has a cylindrical form with radius $w_e = 2\lambda_0$, length $L_e = 3\lambda_0$, and electron number $N_e = 5 \times 10^6$ (density $n_e \approx 1.33 \times 10^{17}$ cm^{-3}). The electron density has a transversely Gaussian and longitudinally uniform distribution.

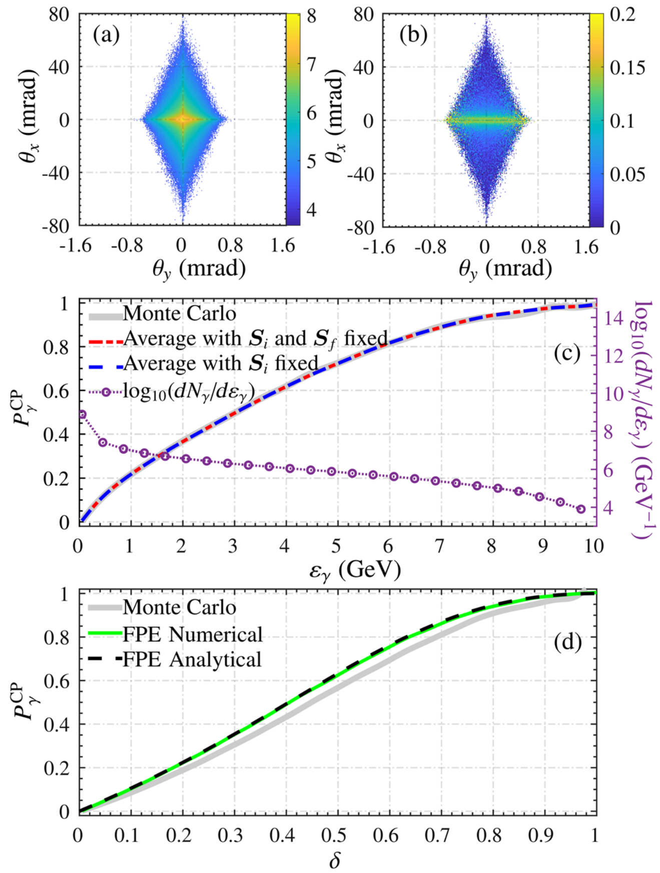

FIG. 2. (a) Angle-resolved photon number density $\log_{10}(d^2N_p/d\theta_x d\theta_y)$(mrad^{-2}) vs deflection angles, $\theta_x = p_x/p_z$ and $\theta_y = p_y/p_z$. (b) Distribution of average circular polarization for all emitted photons $\overline{P^{\mathrm{CP}}} = \overline{\xi_2}$. (c) Degree of circular polarization of γ-photons $P_\gamma^{\mathrm{CP}} = \xi_2$ and energy density of γ photons $\log_{10}(dN_\gamma/d\varepsilon_\gamma)$ vs γ-photon energy ε_γ: via the Monte Carlo method (gray, thick, solid), via the spin-resolved average method of Eq. (6) (red, dash dotted), and via the average method summed up by $\boldsymbol{S}_f$ at each simulation step (blue, dashed), respectively. (d) P_γ^{CP} vs the energy ratio parameter $\delta = \varepsilon_\gamma/\varepsilon_e$: via the Monte Carlo method (gray, thick, solid), and only considering the first photon emission (FPE) calculated numerically (green, thin, solid, using the instantaneous χ parameter) and analytically (black, dashed, employing the constant average parameter of $\chi = 1.41$) via the average method (summing over $\boldsymbol{S}_f$), respectively. In (b) the observation frame can be chosen following [57]. In (c) and (d) the basis vectors of the observation frame $\hat{\mathbf{o}}_1$, $\hat{\mathbf{o}}_2$, and $\hat{\mathbf{o}}_3$ are along the x axis, $-y$ axis, and $-z$ axis, respectively. The laser and other electron beam parameters are given in the text.

The electron initial kinetic energy is $\varepsilon_0 = 10$ GeV, the angular divergence $\Delta\theta = 0.2$ mrad, and the energy spread $\Delta\varepsilon_0/\varepsilon_0 = 0.06$. The emittance of the electron beam is estimated as $\epsilon_e \approx 4\times10^{-4}$ mm mrad. In our simulations, the electron-positron pair creations and their further radiations are taken into account. Such electron bunches are achievable via laser wakefield acceleration [68,69] with further radiative polarization [56], or alternatively, via directly wakefield acceleration of LSP electrons [70].

The angle-resolved number density and average circular polarization of all emitted photons are given in Figs. 2(a) and 2(b). The γ-ray pulse duration is determined by the electron bunch length: $\tau_\gamma \approx \tau_e \approx 10$ fs [40]. The total number of emitted γ photons N_γ at these parameters is about 8.04×10^7 for $\varepsilon_\gamma \geq 1$ MeV and about 1.23×10^7 for $\varepsilon_\gamma \geq 1$ GeV; i.e., N_γ is approximately one order of magnitude larger than N_e, which is in accordance with the analytical estimation $N_\gamma \sim \alpha a_0 N_e \tau/T_0$ [22]. For comparison the polarized γ-photon number in the linear Compton scattering is $N_\gamma/N_e \approx 10^{-3}$ at $\varepsilon_\gamma \approx 56$ MeV [14]. The total flux of the γ rays with $\varepsilon_\gamma \geq 1$ MeV is large due to the shortness of the pulse: $\mathcal{F}_\gamma \approx 8.04\times10^{21}$ s^{-1}. The circular polarization of γ photon $P_\gamma^{\rm CP}$ is proportional to the γ-photon energy ε_γ [derived from Eqs. (2) and (4)], and significantly higher for higher photon energies [see Fig. 2(c)]. Intuitively speaking, the polarization of emitted γ photons (photon helicity in the case of CP) is transferred from the angular momentum (helicity) of electrons. The larger the average energy of emitted γ photons, the smaller the number of emitted photons per electron will be. As the electron carries a certain helicity, the transferred average helicity per photon will be larger in the case of smaller photon number, i.e., in the case of high photon energies. For instance, multi-GeV γ rays of about 10, 8, and 6 GeV can be emitted with circular polarization of about 99%, 94%, and 81%, respectively, and with quite significant brilliances of about 6.25×10^{18}, 3.94×10^{20}, and 1.36×10^{21} photons/(s mm^2 mrad^2 0.1% BW), respectively, which are comparable with the brilliance of unpolarized multi-MeV γ rays obtained in a recent experiment [37]. The detection of vacuum birefringence demands $N_\gamma \sim 10^7$–10^9 CP GeV γ photons [11]. Taking into account that LSP electron bunches with $N_e \approx 5\times10^8$ are feasible [70], we estimate the number of CP γ photons at 4 GeV from Fig. 2(c) for such bunches (using $\Delta\varepsilon_\gamma/\varepsilon_\gamma \sim 0.01$) to reach the required target number for vacuum birefringence $N_\gamma \approx 10^6$ in a single-shot interaction.

Figure 2 indicates that the photon polarization is mostly determined by the incoming electron spin vector $\boldsymbol{S}_i$, where the Monte Carlo and the average methods provide identical results [see Fig. 2(c)]. During multiple photon emissions the average spin of the electron beam from the initial longitudinal direction is gradually oriented along the laser magnetic field in the transverse direction. This effect reduces the circular polarization in the case of multiple photon emissions [see Fig. 2(d)].

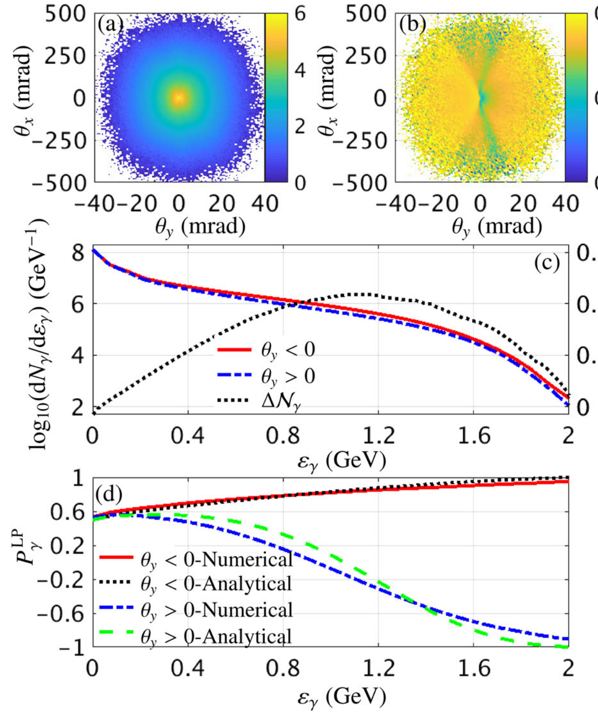

FIG. 3. LP γ-ray emission with a left-handed EP laser with $a_0 = 100$, $\tau = 5T_0$, ellipticity $\epsilon = |E_y|/|E_x| = 0.05$, $\varepsilon_0 = 2$ GeV, initial average spin of electrons $(\bar{S}_x, \bar{S}_y, \bar{S}_z) = (0, 1, 0)$ with 100% polarization, and other laser and electron beam parameters are the same as those in Fig. 2: (a) $\log_{10}(d^2N_p/d\theta_x d\theta_y)$ (mrad^{-2}) vs θ_x and θ_y; (b) Average linear polarization for all emitted photons $\overline{P^{\rm LP}} = \sqrt{\xi_1^2+\xi_3^2}$ vs θ_x and θ_y; (c) $\log_{10}(dN_\gamma/d\varepsilon_\gamma)$ into -10 mrad $< \theta_y < 0$ (red, solid) and into $0 < \theta_y < 10$ mrad (blue, dash dotted), respectively, and the relative difference $\Delta\mathcal{N}_\gamma \equiv (dN_\gamma^{\theta_y<0}/d\varepsilon_\gamma - dN_\gamma^{\theta_y>0}/d\varepsilon_\gamma)/(dN_\gamma^{\theta_y<0}/d\varepsilon_\gamma + dN_\gamma^{\theta_y>0}/d\varepsilon_\gamma)$ (black, dotted) vs ε_γ. (d) Linear polarization of γ photons $P_\gamma^{\rm LP}$ (employing ξ_3) vs ε_γ. In (c) and (d), -10 mrad $< \theta_x < 10$ mrad. The red, solid (blue, dash dotted) and black, dotted (green, dashed) curves indicate the results of -10 mrad $< \theta_y < 0$ ($0 < \theta_y < 10$ mrad), calculated numerically and analytically (with average $\chi \approx 0.7$), respectively. In (d) the basis vectors of the observation frame $\hat{\mathbf{o}}_1$, $\hat{\mathbf{o}}_2$, and $\hat{\mathbf{o}}_3$ are along the x axis, $-y$ axis, and $-z$ axis, respectively.

Generation of LP γ rays is analyzed in Fig. 3. As an unpolarized (or TSP) electron beam head-on collides with a LP laser pulse, an average polarization of about 55% can be obtained [57], which has been pointed out already in [7,46]. However, by harnessing the scheme with an EP laser pulse [56], much higher polarization can be achieved [see Fig. 1(b)]. We focus on the characteristics of the LP γ photons in the high-density region of -10 mrad $< \theta_{x,y} <$ 10 mrad (in this region the total radiation flux $\mathcal{F}_\gamma \approx 2.82\times 10^{21}$ s^{-1} and the average linear polarization $\overline{P^{\rm LP}} \approx 55.2\%$).

Due to the electron-spin-dependence of radiation, namely, that the radiation probability is larger when the electron spin is antiparallel to the rest frame magnetic field [56], the TSP electrons more probably emit photons in the half cycles with $B_y < 0$. In the given EP laser field, the y component of the electron momentum in those half-cycles with $B_y < 0$ is positive, $p_y > 0$, and the corresponding $\theta_y = p_y/p_z < 0$, since $p_z < 0$. Then, the γ photons are more emitted with $\theta_y < 0$, see Fig. 3(c). The relative asymmetry of the photon emission $\Delta\mathcal{N}_\gamma$ corresponds to the relative difference of the radiation probabilities for $\boldsymbol{S}_i$ being parallel and anti parallel to the magnetic field [56] and is most significant around $\varepsilon_\gamma \approx 1.2$ GeV ($\varepsilon_\gamma/\varepsilon_0 \approx 0.6$). Due to radiative electron-spin effects, electrons and γ photons are split into two parts along the minor axis (y axis) of the polarization ellipse [56]. In contrast to the case with unpolarized electrons [7,46], here at emission angles $\theta_y < 0$ ($\theta_y > 0$) the γ-photon polarization is proportional (inversely proportional) to its energy [see Fig. 3(d)]. Thus, specially highly LP γ rays can be obtained in the high-energy region.

For $\theta_y < 0$ in Fig. 3(d), although the average linear polarization of all emitted photons is $\overline{P^{\mathrm{LP}}} \approx 58.3\%$, the high-energy photons achieve even higher linear polarization: at photon energies of about 2, 1, 0.4, and 0.2 GeV, the polarizations are of about 95%, 82%, 70%, and 64%, respectively, and the brilliances of about 8.0×10^{16}, 1.2×10^{20}, 2.9×10^{20}, and 3.5×10^{20} photons/(s mm^2 mrad^2 0.1% BW), respectively. For $\theta_y > 0$, the sign of polarization is energy dependent [57]. Moreover, the depolarization effect due to multiple photon emissions in this case is not significant, because subsequent photon emissions generate LP γ photons as well, see the black, dotted and green, dashed curves in Fig. 3(d). Furthermore, using $N_e \approx 3 \times 10^8$ [70], LP γ photons of $N_\gamma \sim 10^5$–10^6 within $1.015\,\mathrm{GeV} \leq \varepsilon_\gamma \leq 1.021\,\mathrm{GeV}$ ($\Delta\varepsilon_\gamma/\varepsilon_\gamma \approx 0.0059$) can be obtained, which satisfy the requirement ($N_\gamma \gtrsim 6.4 \times 10^4$) of the vacuum birefringence measurement with LP photons [10].

Finally, we have investigated the impact of the laser and electron beam parameters on the polarization of γ rays [57]. Generally, larger energy spread $\Delta\varepsilon_0/\varepsilon_0 = 0.1$, larger angular divergence of 1 mrad, and different collision angles $\theta_e = 179°$ and $\phi_e = 90°$ do not disturb significantly the quality of γ-ray polarization. In generation of CP and LP γ rays, the polarization is robust with respect to the variation of parameters, e.g., τ, ε_0, a_0, and ϵ. As the initial polarization of the electron beam decreases, the polarization of emitted γ photons declines as well.

In conclusion, brilliant multi-GeV CP (LP) γ rays with polarization up to about 95% are shown to be feasible in the nonlinear regime of Compton scattering with ultrarelativistic longitudinally (transversely) spin-polarized electrons. A photon number applicable for vacuum birefringence measurement in ultrastrong laser fields is achievable in a single-shot interaction. A high degree of linear polarization is obtained due to the spin-dependent radiation reaction in a laser field with a small ellipticity, which induces separation of γ photons with respect to the polarization.

We thank J. Evers, T. Wistisen, Y.-S. Huang, R.-T. Guo, and Y. Wang for helpful discussion. Y. Li, F. Wan, and J. Li thank Prof. C. Keitel for hospitality. This work is supported by the National Natural Science Foundation of China (Grants No. 11874295, No. 11804269, and No. 11905169), the National Key R&D Program of China (Grant No. 2018YFA0404801), and the Science Challenge Project of China (Grant No. TZ2016099).

[*]k.hatsagortsyan@mpi-hd.mpg.de
[†]jianxing@xjtu.edu.cn

[1] P. Laurent, J. Rodriguez, J. Wilms, M. Cadolle Bel, K. Pottschmidt, and V. Grinberg, Polarized gamma-ray emission from the galactic black hole cygnus x-1, Science **332**, 438 (2011).
[2] C. Bœhm, C. Degrande, O. Mattelaer, and A. C. Vincent, Circular polarisation: A new probe of dark matter and neutrinos in the sky, J. Cosmol. Astropart. Phys. 05 (2017) 043.
[3] G. Moortgat-Pick *et al.*, Polarized positrons and electrons at the linear collider, Phys. Rep. **460**, 131 (2008).
[4] U. I. Uggerhøj, The interaction of relativistic particles with strong crystalline fields, Rev. Mod. Phys. **77**, 1131 (2005).
[5] J. Speth and A. van der Woude, Giant resonances in nuclei, Rep. Prog. Phys. **44**, 719 (1981).
[6] Z. Akbar *et al.*, Measurement of the helicity asymmetry e in $\omega \to \pi^+\pi^-\pi^0$ photoproduction, Phys. Rev. C **96**, 065209 (2017).
[7] B. King and N. Elkina, Vacuum birefringence in high-energy laser-electron collisions, Phys. Rev. A **94**, 062102 (2016).
[8] A. Ilderton and M. Marklund, Prospects for studying vacuum polarisation using dipole and synchrotron radiation, J. Plasma Phys. **82**, 655820201 (2016).
[9] S. Ataman, M. Cuciuc, L. D'Alessi, L. Neagu, M. Rosu, K. Seto, O. Tesileanu, Y. Xu, and M. Zeng, Experiments with combined laser and gamma beams at ELI-NP, AIP Conf. Proc. **1852**, 070002 (2017).
[10] Y. Nakamiya and K. Homma, Probing vacuum birefringence under a high-intensity laser field with gamma-ray polarimetry at the GeV scale, Phys. Rev. D **96**, 053002 (2017).
[11] S. Bragin, S. Meuren, C. H. Keitel, and A. Di Piazza, High-Energy Vacuum Birefringence and Dichroism in an Ultrastrong Laser Field, Phys. Rev. Lett. **119**, 250403 (2017).
[12] J. P. Bocquet *et al.*, Graal: A polarized -ray beam at esrf, Nucl. Phys. **A622**, c124 (1997).
[13] T. Nakano, H. Ejiri, M. Fujiwara, T. Hotta, K. Takanashi, H. Toki, S. Hasegawa, T. Iwata, K. Okamoto, T. Murakami, J. Tamii, K. Imai, K. Maeda, K. Maruyama, S. Daté, M. M. Obuti, Y. Ohashi, H. Ohkuma, and N. Kumagai, New projects at spring-8 with multi-GeV polarized photons, Nucl. Phys. **A629**, 559 (1998).

[14] T. Omori, M. Fukuda, T. Hirose, Y. Kurihara, R. Kuroda, M. Nomura, A. Ohashi, T. Okugi, K. Sakaue, T. Saito, J. Urakawa, M. Washio, and I. Yamazaki, Efficient Propagation of Polarization from Laser Photons to Positrons Through Compton Scattering and Electron-Positron Pair Creation, Phys. Rev. Lett. **96**, 114801 (2006).

[15] G. Alexander *et al.*, Observation of Polarized Positrons from an Undulator-Based Source, Phys. Rev. Lett. **100**, 210801 (2008).

[16] G. Blanpied *et al.* (LEGS Collaboration), Measurement of $^2h(\rightarrow \gamma, p)n$ with linearly polarized photons in the δ resonance region, Phys. Rev. C **61**, 024604 (1999).

[17] H. Olsen and L. C. Maximon, Photon and electron polarization in high-energy bremsstrahlung and pair production with screening, Phys. Rev. **114**, 887 (1959).

[18] E. A. Kuraev, Yu. M. Bystritskiy, M. Shatnev, and E. Tomasi-Gustafsson, Bremsstrahlung and pair production processes at low energies: Multidifferential cross section and polarization phenomena, Phys. Rev. C **81**, 055208 (2010).

[19] D. Abbott *et al.* (PEPPo Collaboration), Production of Highly Polarized Positrons Using Polarized Electrons at MeV Energies, Phys. Rev. Lett. **116**, 214801 (2016).

[20] D. Lohmann, J. Peise, J. Ahrens, I. Anthony, H.-J. Arends, R. Beck, R. Crawford, A. Hünger, K. H. Kaiser, J. D. Kellie, Ch. Klümper, P. Krahn, A. Kraus, U. Ludwig, M. Schumacher, O. Selke, M. Schmitz, M. Schneider, F. Wissmann, and S. Wolf, Linearly polarized photons at mami (mainz), Nucl. Instrum. Methods Phys. Res., Sect. A **343**, 494 (1994).

[21] V. B. Berestetskii, E. M. Lifshitz, and L. P. Pitaevskii, *Quantum Electrodynamics* (Pergamon, Oxford, 1982).

[22] V. I. Ritus, Quantum effects of the interaction of elementary particles with an intense electromagnetic field, J. Sov. Laser Res. **6**, 497 (1985).

[23] A. Di Piazza, C. Müller, K. Z. Hatsagortsyan, and C. H. Keitel, Extremely high-intensity laser interactions with fundamental quantum systems, Rev. Mod. Phys. **84**, 1177 (2012).

[24] M. Boca and V. Florescu, Thomson and compton scattering with an intense laser pulse, Eur. Phys. J. D **61**, 449 (2011).

[25] I. Ghebregziabher, B. A. Shadwick, and D. Umstadter, Spectral bandwidth reduction of thomson scattered light by pulse chirping, Phys. Rev. ST Accel. Beams **16**, 030705 (2013).

[26] B. Terzić, K. Deitrick, A. S. Hofler, and G. A. Krafft, Narrow-Band Emission in Thomson Sources Operating in the High-Field Regime, Phys. Rev. Lett. **112**, 074801 (2014).

[27] V. N. Baier, V. M. Katkov, and V. M. Strakhovenko, *Electromagnetic Processes at High Energies in Oriented Single Crystals* (World Scientific, Singapore, 1998).

[28] M. L. Ter-Mikaelian, *High Energy Electromagnetic Processes in Condensed Media* (Wiley, New York, 1972), p. 466.

[29] R. Carrigan and J. Ellison, *Relativistic Channeling* (Plenum, New York, 1987).

[30] Yu. A. Chesnokov, V. M. Biryukov, and V. I. Kotov, *Crystal Channeling and its Application at High Energy Accelerators* (Springer, Berlin, 1997).

[31] C. Danson, D. Hillier, N. Hopps, and D. Neely, Petawatt class lasers worldwide, High Power Laser Sci. Eng. **3**, e3 (2015).

[32] S. Gales *et al.*, The extreme light infrastructure nuclear physics (eli-np) facility: New horizons in physics with 10 pw ultra-intense lasers and 20 MeV brilliant gamma beams, Rep. Prog. Phys. **81**, 094301 (2018).

[33] The Extreme Light Infrastructure (ELI), http://www.eli-beams.eu/en/facility/lasers/.

[34] The Vulcan facility, http://www.clf.stfc.ac.uk/Pages/The-Vulcan-10-Petawatt-Project.aspx.

[35] Exawatt Center for Extreme Light Studies (XCELS), http://www.xcels.iapras.ru/.

[36] The Center for Relativistic Laser Science (CoReLS), https://www.ibs.re.kr/eng/sub02_03_05.do.

[37] G. Sarri, D. J. Corvan, W. Schumaker, J. M. Cole, A. Di Piazza, H. Ahmed, C. Harvey, C. H. Keitel, K. Krushelnick, S. P. D. Mangles, Z. Najmudin, D. Symes, A. G. R. Thomas, M. Yeung, Z. Zhao, and M. Zepf, Ultrahigh Brilliance Multi-MeV γ-Ray Beams from Nonlinear Relativistic Thomson Scattering, Phys. Rev. Lett. **113**, 224801 (2014).

[38] J. M. Cole *et al.*, Experimental Evidence of Radiation Reaction in the Collision of a High-Intensity Laser Pulse with a Laser-Wakefield Accelerated Electron Beam, Phys. Rev. X **8**, 011020 (2018).

[39] K. Poder *et al.*, Experimental Signatures of the Quantum Nature of Radiation Reaction in the Field of an Ultraintense Laser, Phys. Rev. X **8**, 031004 (2018).

[40] J.-X. Li, K. Z. Hatsagortsyan, B. J. Galow, and C. H. Keitel, Attosecond Gamma-Ray Pulses via Nonlinear Compton Scattering in the Radiation-Dominated Regime, Phys. Rev. Lett. **115**, 204801 (2015).

[41] J. Magnusson, A. Gonoskov, M. Marklund, T. Zh. Esirkepov, J. K. Koga, K. Kondo, M. Kando, S. V. Bulanov, G. Korn, and S. S. Bulanov, Laser-Particle Collider for Multi-GeV Photon Production, Phys. Rev. Lett. **122**, 254801 (2019).

[42] B. S. Xie, Z. L. Li, and S. Tang, Electron-positron pair production in ultrastrong laser fields, Matter Radiat. Extremes **2**, 225 (2017).

[43] I. I. Goldman, Intensity effects in Compton scattering, Zh. Eksp. Teor. Fiz. **46**, 1412 (1964) [Sov. Phys. JETP **19**, 954 (1964)].

[44] A. I. Nikishov and V. I. Ritus, Quantum processes in the field of a plane electromagnetic wave and in a constant field, Zh. Eksp. Teor. Fiz. **46**, 776 (1964) [Sov. Phys. JETP **19**, 529 (1964)].

[45] C. Bula, K. T. McDonald, E. J. Prebys, C. Bamber, S. Boege, T. Kotseroglou, A. C. Melissinos, D. D. Meyerhofer, W. Ragg, D. L. Burke, R. C. Field, G. Horton-Smith, A. C. Odian, J. E. Spencer, D. Walz, S. C. Berridge, W. M. Bugg, K. Shmakov, and A. W. Weidemann, Observation of Nonlinear Effects in Compton Scattering, Phys. Rev. Lett. **76**, 3116 (1996).

[46] B. King, N. Elkina, and H. Ruhl, Photon polarization in electron-seeded pair-creation cascades, Phys. Rev. A **87**, 042117 (2013).

[47] U. Sinha, C. H. Keitel, and N. Kumar, Polarized Light from the Transportation of a Matter-Antimatter Beam in a Plasma, Phys. Rev. Lett. **122**, 204801 (2019).

[48] D. Yu. Ivanov, G. L. Kotkin, and V. G. Serbo, Complete description of polarization effects in emission of a photon by

an electron in the field of a strong laser wave, Eur. Phys. J. C **36**, 127 (2004).

[49] K. Yokoya, CAIN2.42 Users Manual, https://ilc.kek.jp/~yokoya/CAIN/Cain242/.

[50] C. Sun and Y. K. Wu, Theoretical and simulation studies of characteristics of a compton light source, Phys. Rev. ST Accel. Beams **14**, 044701 (2011).

[51] V. Petrillo, A. Bacci, C. Curatolo, I. Drebot, A. Giribono, C. Maroli, A. R. Rossi, L. Serafini, P. Tomassini, C. Vaccarezza, and A. Variola, Polarization of x-gamma radiation produced by a thomson and compton inverse scattering, Phys. Rev. ST Accel. Beams **18**, 110701 (2015).

[52] G.-P. An *et al.*, High energy and high brightness laser compton backscattering gamma-ray source at ihep, Matter Radiat. Extremes **3**, 219 (2018).

[53] C. P. Ridgers, J. G. Kirk, R. Duclous, T. G. Blackburn, C. S. Brady, K. Bennett, T. D. Arber, and A. R. Bell, Modelling gamma-ray photon emission and pair production in high-intensity laser matter interactions, J. Comput. Phys. **260**, 273 (2014).

[54] N. V. Elkina, A. M. Fedotov, I. Yu. Kostyukov, M. V. Legkov, N. B. Narozhny, E. N. Nerush, and H. Ruhl, Qed cascades induced by circularly polarized laser fields, Phys. Rev. ST Accel. Beams **14**, 054401 (2011).

[55] D. G. Green and C. N. Harvey, Simla: Simulating particle dynamics in intense laser and other electromagnetic fields via classical and quantum electrodynamics, Comput. Phys. Commun. **192**, 313 (2015).

[56] Y.-F. Li, R. Shaisultanov, K. Z. Hatsagortsyan, F. Wan, C. H. Keitel, and J.-X. Li, Ultrarelativistic Electron-Beam Polarization in Single-Shot Interaction with an Ultraintense Laser Pulse, Phys. Rev. Lett. **122**, 154801 (2019).

[57] See Supplemental Material at http://link.aps.org/supplemental/10.1103/PhysRevLett.124.014801 for details on the employed laser fields, on the applied theoretical model, and on the simulation results for other laser or electron parameters.

[58] A. Di Piazza, M. Tamburini, S. Meuren, and C. H. Keitel, Implementing nonlinear compton scattering beyond the local-constant-field approximation, Phys. Rev. A **98**, 012134 (2018).

[59] A. Ilderton, B. King, and D. Seipt, Extended locally constant field approximation for nonlinear compton scattering, Phys. Rev. A **99**, 042121 (2019).

[60] T. Podszus and A. Di Piazza, High-energy behavior of strong-field qed in an intense plane wave, Phys. Rev. D **99**, 076004 (2019).

[61] A. Ilderton, Note on the conjectured breakdown of qed perturbation theory in strong fields, Phys. Rev. D **99**, 085002 (2019).

[62] A. Di Piazza, M. Tamburini, S. Meuren, and C. H. Keitel, Improved local-constant-field approximation for strong-field qed codes, Phys. Rev. A **99**, 022125 (2019).

[63] V. N. Baier, V. M. Katkov, and V. S. Fadin, *Radiation from Relativistic Electrons* (Atomizdat, Moscow, 1973).

[64] W. H. McMaster, Matrix representation of polarization, Rev. Mod. Phys. **33**, 8 (1961).

[65] F. W. Lipps and H. A. Tolhoek, Polarization phenomena of electrons and photons. ii: Results for compton scattering, Physica (Utrecht) **20**, 395 (1954).

[66] Y. I. Salamin and C. H. Keitel, Electron Acceleration by a Tightly Focused Laser Beam, Phys. Rev. Lett. **88**, 095005 (2002).

[67] Y. I. Salamin, G. R. Mocken, and C. H. Keitel, Electron scattering and acceleration by a tightly focused laser beam, Phys. Rev. ST Accel. Beams **5**, 101301 (2002).

[68] W. P. Leemans, A. J. Gonsalves, H.-S. Mao, K. Nakamura, C. Benedetti, C. B. Schroeder, Cs. Tóth, J. Daniels, D. E. Mittelberger, S. S. Bulanov, J.-L. Vay, C. G. R. Geddes, and E. Esarey, Multi-GeV Electron Beams from Capillary-Discharge-Guided Subpetawatt Laser Pulses in the Self-Trapping Regime, Phys. Rev. Lett. **113**, 245002 (2014).

[69] A. J. Gonsalves *et al.*, Petawatt Laser Guiding and Electron Beam Acceleration to 8 GeV in a Laser-Heated Capillary Discharge Waveguide, Phys. Rev. Lett. **122**, 084801 (2019).

[70] M. Wen, M. Tamburini, and C. H. Keitel, Polarized Laser-Wakefield-Accelerated Kiloampere Electron Beams, Phys. Rev. Lett. **122**, 214801 (2019).